Mechanisms of Diffusion of Boron Impurities in SiO_2

Minoru Otani, Kenji Shiraishi, and Atsushi Oshiyama
Institute of Physics, University of Tsukuba, Tennodai, Tsukuba 305-8571, Japan
(Received 19 September 2002; published 21 February 2003)

We report first-principle total-energy calculations that clarify mechanisms of boron diffusion in SiO_2. We find that a B atom takes a variety of stable and metastable geometries depending on its charge state. We also find that atomic rearrangements during the diffusion manifest a wealth of bonding feasibility in SiO_2 and that the calculated activation energy agrees with the experimental data available. Recombination enhanced diffusion is also proposed.

DOI: 10.1103/PhysRevLett.90.075901 PACS numbers: 66.30.Jt, 71.15.Nc, 71.55.–i, 81.65.Mq

Atomic diffusion constitutes fundamental phenomena in materials [1,2]. In semiconductors, for instance, placement of dopant atoms in required regions through diffusion is essential to realize designed performances of devices. Hence a large number of efforts have been made to clarify mechanisms of the atomic diffusion in semiconductors, mainly in Si [3–8].

Semiconductor devices do not consist solely of semiconductors, however. It has been said that were it not for its oxide, Si would lose its premier status in technology: The oxide SiO_2 formed with relative ease insulates Si from the metallic electrode and hereby ensures functions of electronic devices. Yet the guarantee provided by SiO_2 is threatened in current nanometer-scale miniaturization: Leakage current through very thin SiO_2 films has been reported [9,10] and the possible reasons are examined [11,12]; moreover, diffusion of dopant atoms from electrodes, which are usually highly doped polycrystalline Si, and even their penetration through SiO_2 films have become serious [13]. It is thus urgent to clarify atom-scale mechanisms of the dopant diffusion in SiO_2.

SiO_2 is an ambivalent material, both covalent and ionic: A Si atom is coordinated with four oxygen atoms with sp^3 hybridization, whereas the O atom substantially attracts electrons from nearby Si atoms. Although SiO_2 exhibits a variety of polymorphs, this situation is common even in amorphous SiO_2. Diffusion is the sequence of cooperative atomic reactions in which covalent bonds are rearranged as a diffusing species migrates. The probable rearrangements are determined by total-energy surfaces that may be sensitive to the local charge distribution around the diffusing species. Diffusion of a foreign atom in ambivalent SiO_2, which has not been focused in the past [14,15], is therefore of interest also from scientific viewpoints.

In this Letter, we have performed total-energy calculations to clarify mechanisms of B diffusion in SiO_2. We have found that the B impurity has a variety of stable and metastable atomic geometries depending on its charge state, exhibiting negative-U characters. Diffusion pathways from those stable geometries and corresponding activation energies are also found to be sensitive to the charge state. Detailed examination of atomic geometries during the diffusion unravels surprisingly rich chemical feasibility of the constituent elements. The calculated activation energies agree with experimental data.

The density-functional theory is used within the generalized-gradient approximation [16–18]. Norm-conserving pseudopotentials for Si [19] and ultrasoft pseudopotentials for O and B [20] are adopted to describe the electron-ion interaction. As a representative of SiO_2, we consider α-quartz [21]. The supercell containing 72 lattice sites is used to simulate a B impurity in an otherwise perfect SiO_2. The cutoff energy of the plane-wave basis set is 25 Ry. We use the Γ point for the Brillouin zone (BZ) sampling [22]. Geometries are optimized for all atoms until the remaining force on each atom is less than 5 mRy/Å. The diffusion pathways and activation energies for the B impurity are calculated by the constrained optimization in a $(N-1)$-dimensional space [23], where N is the ionic degrees of freedom in a unit cell. For the charged states, a monopole model [12] is used to correct the total-energy lowering due to spurious Coulomb interactions in the supercell model.

We have performed an extensive search for stable geometries of B in SiO_2 and found charge-state dependent multistability. Figure 1 shows stable and metastable geometries of B in SiO_2. In the most stable geometry $B_SSi_{(3)}$ [Fig. 1(a)] with the neutral charge state, B and Si atoms take a split-interstitial configuration around the original Si site and, surprisingly, the Si atom becomes threefold coordinated. We have also found other metastable geometries B_{ox} [Fig. 1(b)], $B_OSi_{(5)}$ [Fig. 1(c)], and B_OO_i [Fig. 1(d)]. In B_{ox}, which is higher than $B_SSi_{(3)}$ in total energy by 0.09 eV, a B atom intervenes between Si and O atoms and is twofold coordinated. When the B and the neighboring O are exchanged in B_{ox}, we reach another metastable geometry B'_{ox}, higher than B_{ox} in energy by 0.24 eV. In $B_OSi_{(5)}$, which is higher than $B_SSi_{(3)}$ in energy by 0.21 eV, a B atom substitutes for an O atom, the dislodged O atom forms a weak bond with another Si atom, and this Si becomes fivefold coordinated (floating bond [24]). Another floating bond configuration B_OO_i in which B and the dislodged O are bonded to the Si and

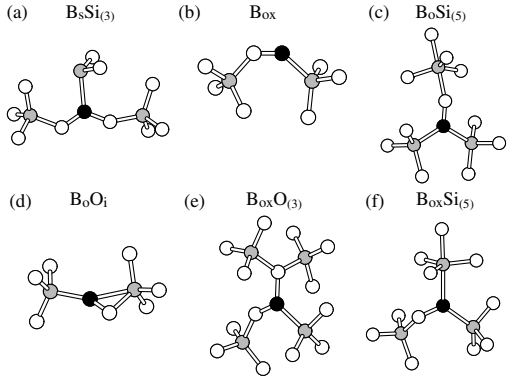

FIG. 1. Stable and metastable atomic geometries of a B impurity in SiO_2. The $B_SSi_{(3)}$ (a), B_{ox} (b), $B_OSi_{(5)}$ (c), B_Oi (d), $B_{ox}O_{(3)}$ (e), and $B_{ox}Si_{(5)}$ (f) geometries. White, gray, and black balls indicate O, Si, and B atoms, respectively. Only a part of the atoms in a unit cell are shown to avoid visual complexity.

thereby form a floating bond is also found to be metastable but 0.53 eV higher in energy than $B_SSi_{(3)}$. Obtained stability of $B_SSi_{(3)}$ is interpreted in terms of bond strength: In $B_SSi_{(3)}$ there is a Si dangling bond, whereas in B_{ox} a B dangling bond; the total-energy difference of 0.09 eV between $B_SSi_{(3)}$ and B_{ox} is comparable with the bond energy difference, $\varepsilon_{\text{Si-O}} = 8.29$ eV and $\varepsilon_{\text{B-O}} = 8.38$ eV [25].

Analyses of Kohn-Sham levels clarify that a deep level appears in the gap for each of the (meta)stable geometries with the neutral charge state. An electron is accommodated in the deep level so that the spin is 1/2. Yet the characters are different from each other: the Si dangling bond in $B_SSi_{(3)}$, the B dangling bond in B_{ox}, and the antibonding character between the O-nonbonding and the B-Si bonding states in $B_OSi_{(5)}$.

Energetics depends on the charge state. For positively charged ($+1$) state, $B_OSi_{(5)}$ and B_Oi geometries become unstable. The most stable geometry is $B_{ox}O_{(3)}$ in Fig. 1(e) in which a B atom intervenes between Si and O atoms, and then forms the third bond with the nearby O atom. A missing electron in the $+1$ state causes two electrons of the nonbonding state of the nearby O to assist in the formation of the third bond with B. B_{ox} and $B_SSi_{(3)}$ geometries are found to be metastable and are higher than $B_{ox}O_{(3)}$ in total energy by 0.74 and 0.50 eV, respectively. For the negatively charged (-1) state, the B_{ox} and $B_{ox}O_{(3)}$ become unstable. We have found that $B_OSi_{(5)}$ geometry in Fig. 1(c) is the most stable geometry. An additional electron is effective to strengthen the floating bond around Si and stabilizes $B_OSi_{(5)}$. As a metastable geometry we have found $B_SSi_{(3)}$ and $B_{ox}Si_{(5)}$ [Fig. 1(f)] which are higher than $B_OSi_{(5)}$ in total energy by 0.77 and 1.32 eV, respectively.

In the neutral state, there are several metastable geometries of which energies are close to that of the most stable. In negatively or positively charged states, on the other hand, the energy of the most stable geometry is substantially lower than those of other metastable geometries. This is owing to a fact that the missing or the additional electron is effective in forming the peculiar bond configuration in each charged state. This charge-state-dependent chemical feasibility has important consequences in the B diffusion explained below.

The stability among different charge states in their equilibria is obtained by comparing $\Omega(Q, \mu) \equiv E(Q) + Q\mu$, where $E(Q)$ is the total energy of the charge state Q, and μ is the electron chemical potential, i.e., the Fermi level in the energy gap. Figure 2 shows $\Omega(Q, \mu)$ for some of the (meta)stable geometries of the B impurity explained above as a function of μ for the positive ($+1$; $Q = 1$), neutral (0; $Q = 0$), and negative (-1; $Q = -1$) charge states. The μ value $\mu_{\text{th}}(Q/Q + 1)$, at which $\Omega(Q, \mu) = \Omega(Q + 1, \mu)$, determines the relative stability of the Q and $(Q + 1)$ charge states and is called the thermodynamic level [12]. Figure 2 clearly shows that positively charged or negatively charged states are stable, whereas the neutral charge state is metastable for any value of μ in the energy gap. Hence the B in SiO_2 is a

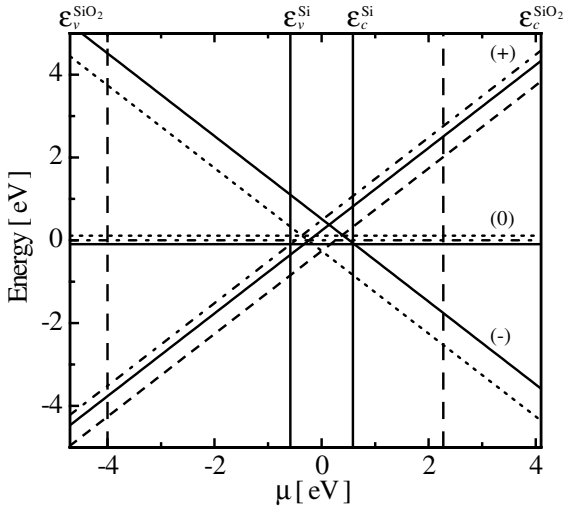

FIG. 2. Relative formation energies $\Omega(Q, \mu)$ of several stable geometries of the B impurity as a function of the electron chemical potential μ in the energy gap of SiO_2: $B_SSi_{(3)}$ (solid lines), $B_OSi_{(5)}$ (dotted lines), B_{ox} (dash-dotted lines), and $B_{ox}O_{(3)}$ (dashed lines). The energies for the positive ($+$), neutral (0), and negative ($-$) charge states are shown. Both ends of μ are the experimental valence band top ($\varepsilon_v^{SiO_2}$) and conduction band bottom ($\varepsilon_c^{SiO_2}$) of SiO_2. Those of Si (ε_v^{Si} and ε_c^{Si}) are denoted by vertical lines. The density-functional $\varepsilon_v^{SiO_2}$ and $\varepsilon_c^{SiO_2}$ are shown as a reference by vertical dashed lines near both ends of μ. These alignments are done by matching the theoretical and experimental thermodynamic levels [26] related to the interstitial H in SiO_2, which is known to be located at 0.2 eV above the center of the Si gap (the energy reference here), and by using the valence-band offset of 4.3 eV between SiO_2 and Si (refer to [12] for details).

negative-U system associated with structural transformation. The energy cost to render the charged states neutral is found to be 0.2–0.8 eV when μ is in the region of the Si energy gap.

We are now in a position to discuss the diffusion. We start with the most stable geometry and explore a variety of possible diffusion pathways toward the final geometry [27] using our constrained minimization technique. The most favorable pathways and corresponding activation energies determined by the present calculations are shown in Fig. 3. We have found that the B atom diffuses along bond networks of SiO_2 irrespective of its charge state, deforming and breaking a bond configuration, and then forming a next favorable bond configuration. In the +1 state, starting from $B_{ox}O_{(3)}$, the B takes the metastable geometry of B'_{ox}, diffuses through the saddle point (see below) towards another metastable B_{ox}, breaks and reforms several configurations, and then diffuses to the final $B_{ox}O_{(3)}$ geometry again through the B'_{ox}. In the −1 state, the B starts from the initial $B_OSi_{(5)}$, passes through the saddle point (see below), and reaches the nearby $B_OSi_{(5)}$. Yet this $B_OSi_{(5)}$ is still the halfway point. To proceed farther from the initial $B_OSi_{(5)}$, the B takes another metastable $B_{ox}Si_{(5)}$ and then reaches the final geometry. When the B is in the neutral state, rearrangements of several bonding configurations are again required to reach the final geometry. Yet activation energy for the diffusion of neutral B is substantially lower than those for charged B: The calculated barriers for the neutral B is 0.8 eV, whereas those for the +1 and the −1 states are 2.3 and 2.2 eV, respectively. This is due to the charge-state-dependent chemical feasibility stated above.

Variation of atomic geometries during the diffusion is extremely interesting and further elucidates the importance of the charge state. The saddle point for the +1 state lies between the B_{ox} and the B'_{ox} geometries and is shown in Fig. 4(a). The barrier determining process for the +1 state is the exchange process between B and O atoms, and this process, as is evident from Fig. 4(a), costs substantial energy. The saddle point for the −1 state is shown in Fig. 4(b) where the Si atoms around B form several floating bonds. It is found that an additional electron is shared consecutively by various floating bonds during the diffusion (not shown here). However, the total energy of the saddle-point geometry is much higher than the most stable $B_OSi_{(5)}$.

In the neutral state, the B diffusion requires the same structural transformation between B_{ox} and B'_{ox} as in the +1 state (Fig. 3). Yet the barrier is dramatically low, more than 1.5 eV lower than for the +1 state. Figure 4(c) clarifies the origin. For the neutral state, multiple bonds among B, O, and Si atoms are formed in the saddle-point geometry. This multiple-bond configuration in the neutral state is close to the metastable geometry B_OO_i [Fig. 1(d)] which is unstable for the +1 state. An electron which triggers the diffusion reaction toward the favorable saddle point in the neutral state is missing in the +1 state.

Our calculations indicate that the +1 or −1 charged state is more stable than the neutral state for any position of μ in the gap (Fig. 2). It is thus concluded that the diffusion barrier is 2.2–2.3 eV in usual situations. This theoretical value agrees well with the experimental values [28].

In nonequilibrium conditions, however, we expect recombination enhanced diffusion. When μ is in the region of Si energy gap, the total-energy difference between neutral and charged states is less than 1 eV. Starting from the +1 charged $B_{ox}O^{+1}_{(3)}$ geometry, for instance, the B atom becomes B'^{+1}_{ox} geometry. We have determined

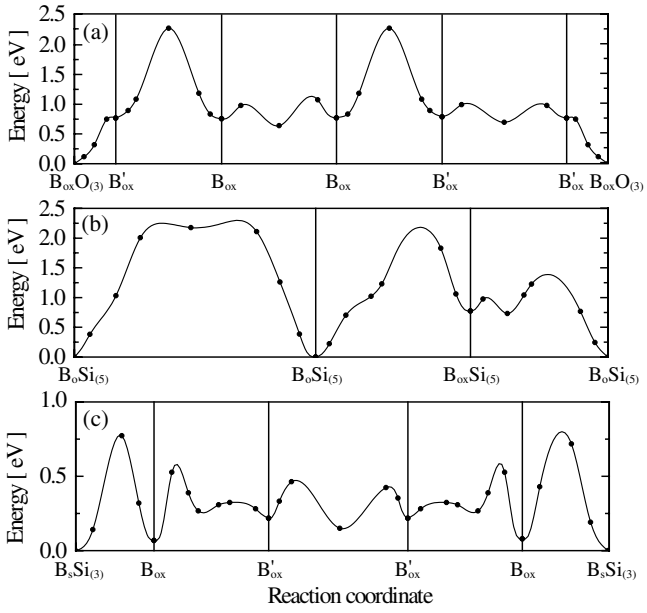

FIG. 3. Total energy variations along diffusion pathways: the $B_{ox}O_{(3)} \rightarrow B_{ox}O_{(3)}$ path with positively charged (a), the $B_OSi_{(5)} \rightarrow B_OSi_{(5)}$ path with negatively charged (b), and the $B_SSi_{(3)} \rightarrow B_SSi_{(3)}$ path with neutral (c) states. The left and right ends correspond to the initial and the final geometries. The vertical lines denote intermediate metastable geometries.

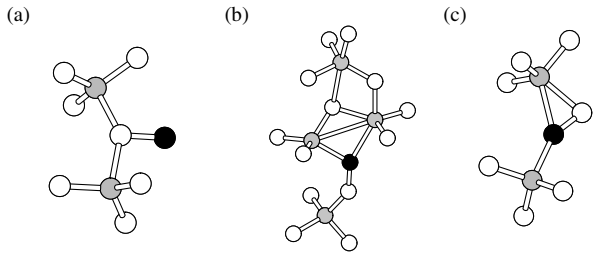

FIG. 4. Saddle-point geometries during the B diffusion for the +1 charged state (a) and the −1 charged state (b). A saddle-point geometry between B_{ox} and B'_{ox} for the neutral state is also shown in (c). White, gray, and black balls indicate O, Si, and B atoms, respectively. Only a part of atoms in a unit cell are shown to avoid visual complexity.

the reaction pathway $B_{ox}O^{+1}_{(3)} \rightarrow B'^{+1}_{ox}$ and obtained the energy barrier of 0.8 eV. Upon electron capture at the B'^{+1}_{ox} geometry (intuitively, capture at the B dangling bond), B'^{+1}_{ox} becomes neutral B'_{ox} and migrates with the energy barrier of 0.5 eV [Figs. 3(a) and 3(c)]. The neutral B'_{ox} can be positive upon hole capture at some point and becomes the +1 charged B'^{+1}_{ox} and then $B_{ox}O^{+1}_{(3)}$. The net activation energy involves the energy gain to capture an electron at the geometry B'_{ox}. It is 0.0–0.5 eV from Fig. 2. Then the diffusion barrier for this whole recombination process is 0.8–1.3 eV. Similarly, for the negatively charged state the reaction, $B_OSi^{-1}_{(5)} \rightarrow B_SSi^{-1}_{(3)} \rightarrow B_SSi^{0}_{(3)} \cdots B_SSi^{0}_{(3)} \rightarrow B_SSi^{-1}_{(3)} \rightarrow B_OSi^{-1}_{(5)}$, substantially enhances the diffusion. We have obtained the energy barrier of 1.0–1.6 eV for this reaction.

In summary, we have presented first-principle calculations that clarify mechanisms of the B diffusion in SiO_2. The results clearly show characteristic features of the diffusion of a foreign atom in the ambivalent material which is both covalent and ionic. The charge-state-dependent feasibility of bond formations is the principal factor of the atomic diffusion.

Computations were done at the SIPC, University of Tsukuba, and at RCCS, Okazaki National Institute. The work was supported partly by Grant-in-Aid from MEXT Japan under Contracts No. 14550020 and No. 14550021, and by the ACT-JST project.

[1] W. Frank, U. Gösele, H. Mehrer, and A. Seeger, in *Diffusion in Crystalline Solids*, edited by G. E. Murch and A. S. Nowick (Academic, New York, 1984).
[2] P. M. Fahey, P. B. Griffin, and J. D. Plummer, Rev. Mod. Phys. **61**, 289 (1989).
[3] R. Car, P. J. Kelly, A. Oshiyama, and S. T. Pantelides, Phys. Rev. Lett. **52**, 1814 (1984); **54**, 360 (1985).
[4] C. S. Nichols, C. G. Van de Walle, and S. T. Pantelides, Phys. Rev. Lett. **62**, 1049 (1989); Phys. Rev. B **40**, 5484 (1989).
[5] K. C. Pandey, Phys. Rev. Lett. **57**, 2287 (1986); K. C. Pandey and E. Kaxiras, Phys. Rev. Lett. **66**, 915 (1991).
[6] P. E. Blöchl *et al.*, Phys. Rev. Lett. **70**, 2435 (1993).
[7] H. Bracht, E. E. Haller, and R. Clark-Phelps, Phys. Rev. Lett. **81**, 393 (1998).
[8] A. Ural, P. B. Griffin, and J. D. Plummer, Phys. Rev. Lett. **83**, 3454 (1999).
[9] J. Maserijian and N. Zamani, J. Appl. Phys. **53**, 559 (1982).
[10] G. J. Hu and R. H. Bruce, IEEE Trans. Electron Devices **32**, 584 (1985).
[11] A. Oshiyama, Jpn. J. Appl. Phys. **37**, L232 (1998).
[12] P. E. Blöchl and J. H. Stathis, Phys. Rev. Lett. **83**, 372 (1999).
[13] J. R. Pfiester *et al.*, IEEE Trans. Electron Devices **37**, 1842 (1990). Successful fabrication of 1.3-nm gate oxides is recently reported: G. Timp *et al.*, *IEDM Technical Digest* (Institute of Electrical and Electronics Engineers, Piscataway, NJ, 1997), p. 930; T. Sorsch *et al.*, in *Proceedings of the Symposium on VLSI Technology, Digest of Technical Papers* (Institute of Electrical and Electronics Engineers, Piscataway, NJ, 1998), p. 222.
[14] Some models for B diffusion in SiO_2 is proposed by compiling thermochemical data: R. B. Fair, J. Electrochem. Soc. **144**, 708 (1997).
[15] Oxygen diffusion in SiO_2 is examined by density-functional calculations: D. R. Hamann, Phys. Rev. Lett. **81**, 3447 (1998); Y.-G. Jin and K. J. Chang, Phys. Rev. Lett. **86**, 1793 (2001).
[16] J. P. Perdew, K. Burke, and M. Ernzerhof, Phys. Rev. Lett. **77**, 3865 (1996); J. P. Perdew, K. Burke, and Y. Wang, Phys. Rev. B **54**, 16 533 (1996).
[17] Codes used in the present work are based on Tokyo Ab initio Program Package (TAPP) developed by us; see J. Yamauchi, M. Tsukada, S. Watanabe, and O. Sugino, Phys. Rev. B **54**, 5586 (1996); H. Kageshima and K. Shiraishi, Phys. Rev. B **56**, 14 985 (1997); O. Sugino and A. Oshiyama, Phys. Rev. Lett. **68**, 1858 (1992).
[18] The inclusion of spin degree of freedom is important: The total-energy gain due to spin polarization is typically 0.2–0.5 eV, and the spin splittings of Kohn-Sham levels are 1.5–2.0 eV.
[19] N. Troullier and J. L. Martins, Phys. Rev. B **43**, 1993 (1991).
[20] D. Vanderbilt, Phys. Rev. B **41**, 7892 (1990).
[21] B diffusion in another polymorph, α-cristobalite, has also been examined. We use the 72-site supercell and focus the positively charged B. It is found that the stable and saddle-point geometries in α-cristobalite are essentially the same as those in α-quartz. The calculated activation energy for B^{+1} in α-cristobalite is smaller than that in α-quartz by less than 0.3 eV. This energy difference comes from the structural difference in the global bonding network between cristobalite and quartz. It is thus expected that the diffusion barrier may change by such an amount in amorphous SiO_2.
[22] The convergence of the calculational parameters are examined by using the cutoff energies of 25, 49, and 64 Ry, and the Γ point and the 8 k point samplings in BZ. The calculated total-energy differences are found to converge within 0.02 eV.
[23] S. Jeong and A. Oshiyama, Phys. Rev. Lett. **81**, 5366 (1998).
[24] S. T. Pantelides, Phys. Rev. Lett. **57**, 2979 (1986).
[25] *CRC Handbook of Chemistry and Physics*, edited by D. R. Lide (CRC Press, Florida, 2000), 81st ed.
[26] S. Jeong and A. Oshiyama, Phys. Rev. Lett. **86**, 3574 (2001).
[27] The final geometry is one of nearby most stable geometries from which B repeat the process to diffuse in the long distance. In the case of α-quartz, the final geometry is obtained from the starting geometry by a threefold rotation followed by a $2c/3$ nonprimitive translation.
[28] The experimental barrier for the B diffusion scatters between 2–3 eV. See, e.g., T. Aoyama, H. Tashiro, and K. Suzuki, J. Electrochem. Soc. **146**, 1879 (1999), and references therein.